To cite this version : Loubiere, Karine and Oelgemoeller, Michael and Aillet, Tristan and Dechy-Cabaret, Odile and Prat, Laurent E. *Continuous-Flow Photochemistry: a need for chemical engineering.* (2016) Chemical Engineering and Processing: Process Intensification, vol. 104. pp. 120-132. ISSN 0255-2701

Continuous-flow photochemistry: A need for chemical engineering

Karine Loubière[a,b,*], Michael Oelgemöller[c], Tristan Aillet[a,b], Odile Dechy-Cabaret[a,d], Laurent Prat[a,b]

[a] CNRS, Laboratoire de Génie Chimique (LGC UMR 5503), 4 allée Emile Monso, BP 84234, 31432 Toulouse, France
[b] Université de Toulouse, INPT, ENSIACET, F-31432 Toulouse, France
[c] James Cook University, College of Science, Technology and Engineering, Townsville, Queensland 4811, Australia
[d] CNRS, Laboratoire de Chimie de Coordination (LCC UPR 8241), 205 route de Narbonne, BP 44099, F-31077 Toulouse, France

A B S T R A C T

The present paper aims to illustrate that chemical engineering enables to address some of the current challenges and issues in continuous-flow photochemistry. For that, some common limitations encountered in industrial photochemistry are firstly highlighted and a general overview on flow photochemistry equipment is presented. The main challenges linked to photochemical (micro)reactor engineering are subsequently stated. By considering only the case of a purely direct photochemical reactions $A \xrightarrow{h\upsilon} B$ in homogenous medium, the key factors to consider when implementing such photochemical reactions in microstructured technologies are outlined. Their influence on the outputs (conversion, productivity, photonic efficiency) of this simple type of photochemical reaction is then discussed. The significance of chemical engineering frameworks is finally demonstrated using several examples concerning the understanding of the coupling between the different phenomena involved, the predictions of the performances obtained, the acquisition of kinetics data and the elaboration of strategies for photochemical process intensification and smart scale-up. In the future, the challenge will be to integrate the complexity of photochemistry (e.g. heterogeneous phase reactions) into the present modelling tools so as to enlarge the spectrum of strategies devoted to photochemical process intensification.

1. Introduction

Organic photochemistry has the potential to emerge as a key synthesis pathway in sustainable chemistry. In recent years, photochemical reactions have significantly enriched the methodology of organic synthesis [1–4]. In contrast to thermal reactions, photochemical reactions are induced via the electronically excited state possessing a different electron configuration than their corresponding thermal ground states [5–8]. Consequently, the chemical reactivity of excited molecules is considerably different from that of ground state molecules. The following points are particularly interesting in the context of sustainability: (i) multistep syntheses of complex molecules are shortened and simplified; often, a high molecular complexity is generated in one step from simple precursors, (ii) a portfolio of novel compound families (e.g. strained rings) is becoming accessible or more easily accessible,

and (iii) in many reactions, the photon acts as a "traceless reagent", and no chemical catalysts (acid, base, metal, etc.) or activating groups are needed [9–11]. The 12 guiding principles of Green Chemistry [12,13] are thus addressed by photochemistry. In addition, photochemical reactions are currently becoming an indispensable tool in the search of new biologically active compounds for applications in medicine, fine chemical and pharmaceutical industries, as well as in many other fields (e.g. material and environmental sciences) [14–23].

At the same time, continuous-flow technologies, in particular microstructured reactors, have emerged as alternatives to batch processing and their implementation in process intensification strategies is likewise crucial for sustainable chemistry [24]. Recently, various works have shown that these technologies are also suitable and beneficial for preparative photochemistry [25–31], boosting the interest in continuous-flow photochemistry.

The present paper aims to illustrate that some of the current challenges and issues in continuous-flow photochemistry can be addressed using a chemical engineering framework. Such a framework is indeed essential to elaborate a process intensification strategy which enables adaptation of the microstructured

---

* Corresponding author at: CNRS, Laboratoire de Génie Chimique (LGC UMR 5503), 4 allée Emile Monso, BP 84234, 31432 Toulouse, France.
  E-mail address: Karine.Loubiere@ensiacet.fr (K. Loubière).

photoreactor design (channel design, dimensions, light source, etc.) to photochemical reaction specificities, and more generally a transfer from batch to continuous mode operations.

Firstly, the common limitations encountered in industrial photochemistry will be identified and a general overview on flow photochemistry equipment presented (Section 2). The main challenges linked to photochemical (micro)reactor engineering will then be exposed (Section 3). By considering only the case of purely direct photochemical reactions $A \xrightarrow{h\upsilon} B$ occurring in homogenous medium, the key factors to consider when implementing such a photochemical reaction in microstructured technologies will be outlined basing on modeling considerations (Section 4). In the last section (Section 5), some examples will be presented to illustrate, for this particular case of a photochemical reaction, how a chemical engineering framework enables to understand and formalize the positive effect of microstructured technologies for photochemistry.
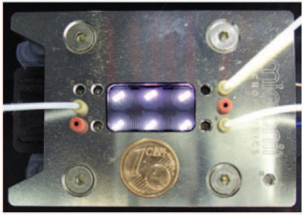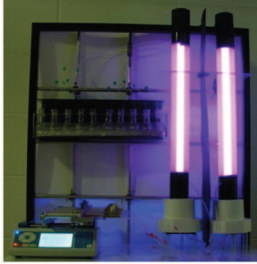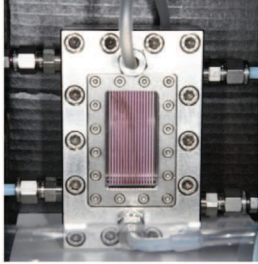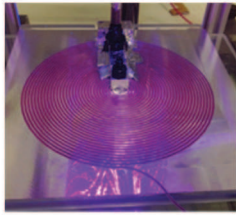
2. Industrial photochemistry: a «renaissance»?

Since 1975, 8000 photochemical reactions for organic synthesis have been referenced [32]. Despite this huge portfolio, organic photochemistry has not found widespread implementations in chemical industry [33,34]. It is difficult to obtain a global overview on currently existing photochemical activities as industrial processes are often kept confidential. Nevertheless, it is known that many industrial photoreactions have been established decades ago and have since been operational largely unchanged [35]. Based on the information available by Braun et al. [34], the worldwide electrical power installed for the radiation sources used in preparative photochemical equipment represents almost 30 MW, thus demonstrating its significant importance. Photochemical synthesis is mostly applied by chemical companies that produce intermediate and/or fine chemicals (e.g. pharmaceutical, agrochemical, food processing and fragrance industries) and by companies producing basic or final products (e.g., food, electronic, automotive, furniture, building and packaging industries). It should be noted that the production of highly priced fine chemicals (e.g. fragrance, pharmaceutically active compounds) represents the minor fraction of the installed electrical power previously mentioned [34]. Among the well-known examples of industrial photochemistry, one can mention the synthesis of vitamin D_3 and vitamin A (BASF, Hoffmann-LaRoche), the photooximation of cyclohexane (Toray), the photochlorination of toluene, the synthesis of rose oxide (Symrise) [36] and more recently the synthesis of artemisinin [37].

The reluctance to transfer preparative photochemistry to large-scale is mainly due to the limitations of the currently available technology, which requires outdated immersion-type reactors, often operating in semi-batch mode (circulation of the reaction medium between a large central reservoir and the reactor), equipped with expensive and energy-demanding mercury lamps. In these installations, process limitations are numerous due to the uncontrolled coupling between hydrodynamics, light, mass transfer and photochemical kinetics. As a result, lower selectivity and yields than on lab-scale are commonly obtained. Many of these systems furthermore need optical filters to cut off undesired radiation, large dilutions to overcome unfavorable light absorption and intensive cooling to counter the heat generation by the lamps.

By combining the benefits of micro-scale with continuous-flow mode, microstructured reactors enable, when compared to conventional photochemical equipment, higher conversions and selectivities while reducing irradiation time [25–31]. Some of their specific advantages are: (i) extensive penetration of light, even for concentrated chromophore solutions, (ii) minimization of side reactions or decompositions by flow-operation, (iii) easy control of the irradiation time and (iv) safer conditions (for example when involving heat-sensitive oxygenated intermediates). The combination of microstructured technology with new light sources (e.g. Light-Emitting Diodes (LED) or excimer lamps) additionally offers promising perspectives in terms of energy-savings [38]. Consequently, there is at present an increasing interest in continuous-flow photochemistry, leading to a "renaissance" of preparative photochemistry. Most studies are dedicated to the production of small quantities in often improvised 'in house'-made reactors (Fig. 1a). The results obtained have nevertheless strengthened this technology and have sparked the development of dedicated and more advanced equipment. Currently, commercial technologies (e.g. from the companies YMC [39], Mikroglas [40], Ehrfeld [41], Future Chemistry [42]) (Fig. 1b) and internally developed reactors [43–45] mainly enable continuous-flow photochemistry on lab-scales, although isolated examples of meso-scale photoreactions in flow have been reported as well. However, a scale-up to industrially relevant amounts, i.e. above a few hundred kilograms per year, has not been realized yet. Thus far, very few flow photoreactors are available for several grams per day (Vapourtec UV-150 [46]) or kilogram per day operations (Corning® G1 Photo Reactor [47], Heraeus Noblelight [48]) (Fig. 1b). A flow-photochemical production facility for the synthesis of low-volume anticancer compounds has recently been erected by Heraeus Noblelight [48], thus demonstrating the potential of this emerging new technology.

(a) Examples of improvised 'in house'-made microreactors,

Microchip device (Micronit Microfluidics FC_R150.676.2) [49]	Multicapillary tower device [50]	Falling film device (IMM FFMR-Standard) [51]	Spiral-shaped device [54, 55]
(Borofloat glass chip, UVA-LED-driven)	(FEP tubing, UVA fluorescent tube)	(metal reaction plate, visible compact fluorescent bulb)	(FEP tubing, LED-driven)

(b) examples of commercial microstructured technologies
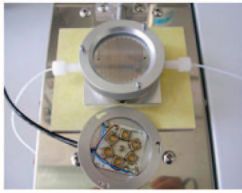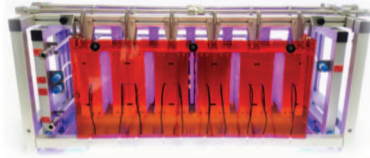
Future Chemistry (PhotoChemistry module®) [42]	YMC KeyChem Lumino® [39]	Vapourtec easy-Photochem [46]	Corning® G1 Photo Reactor [47]
(glass chip, cooling unit, LED-driven)	(metal reaction plate, cooling unit, LED-driven)	(tube device, irradiated from inside with tunable 150 W Hg-lamp, cooling unit)	(concept of plate heat-exchangers, 5 units in series, LED-driven)

Fig. 1. Microstructured technologies for preparative photochemistry: (a) examples of improvised 'in house'-made microreactors, (b) examples of commercial microstructured technologies [49,50].

Microstructured technologies thus provide new scientific and technological solutions (i) for overcoming problems of mass and photonic transfers encountered in classical photochemical units, (ii) for optimizing photochemical reaction protocols and (iii) for their subsequent implementation in meso-scale continuous-flow reactors under greener, safer and resource-efficient and energy-efficient conditions. Despite this huge potential, there are at present few attempts (i) to understand the positive effects of the small-scale on the photochemical reaction performances, (ii) to predict the reaction outputs at the outlet of the microphotoreactor and/or (iii) to compare the performances obtained in microstructured technologies with the ones in conventional equipment [27–31]. This research gap is yet essential for implementing photochemical reactions in intensified continuous-flow processes compatible with an industrial production, and for addressing issues related to batch-to-continuous transfer and smart scale-up.

Motivated by this perspective, our previous work proposed, for a purely direct photochemical reactions $A \overset{h\upsilon}{\rightarrow} B$ occurring in homogenous medium, different modeling approaches (one- or two-dimensional, taking into account, if necessary, the

polychromatic character of the light source) to predict the conversion at the microreactor outlet [47,53], to establish some guidelines to avoid mass-transfer limitations in microphotoreactors [54] or to acquire some kinetics data on photochemical reactions [56]. This modelling background will constitute the basis of the chemical engineering approach presented in the following sections to address current challenges and issues in continuous-flow-photochemistry.

3. Challenges linked to photochemical (micro)reactor engineering

As for thermal reactions, the starting point for photo(micro) reactor engineering is the law describing the kinetics of the photochemical reaction. This law is not always easy to express, in particular when heterogeneous photoreaction systems are involved or when photochemical and thermal steps are combined. For illustration purposes, a purely photochemical transformation $A \xrightarrow{h\upsilon} B$ is considered here. The kinetic rate is expressed, at a given location in the microreactor and at a given wavelength λ, as:

$$r_{A,\lambda} = \phi_\lambda \times e^a_{A,\lambda} \tag{1}$$

where ϕ_λ is the quantum yield of the reaction (mol mol photon^{-1}) and $e^a_{A,\lambda}$ the local volumetric rate of photon absorption of the species A (mol photon m^{-3} s^{-1}). These two parameters are spectral physical quantities.

Several variants for the definition of **quantum yield** can be encountered, depending whether it is related to the primary photochemical process or to the overall process [33]. However, it can be reasonably defined as the ratio between the molar flux of molecules reacting during the photochemical reaction and the flux of photons absorbed by the molecule. This key parameter provides information on the reaction mechanism: $\phi_\lambda > 1$ means that it is a chain reaction (the photochemical step solely initiates the reaction), and $\phi_\lambda < 1$ that it is a quasi-stoechiometric reaction in which some deactivation processes occur (as described by the Jablonski's diagram) or some other reactions (including quenching mechanisms) are in competition with the photochemical step. For example, when considering sensitized photooxygenations, the expression of this quantum yield becomes more complicated due to the contributions of the quantum yield for the formation of the triplet state of the sensitizer, of the efficiency of the energy transfer from the sensitizer to form singlet oxygen and of the efficiency of the formation of the product from singlet oxygen [33].

It is important to differentiate the quantum yield from the chemical yield. For example, a high chemical yield can be obtained with a low quantum yield, but these reactions would require long irradiation times.

The second parameter involved in Eq. (1) is the **local volumetric rate of photon absorption of the species A**, $e^a_{A,\lambda}$. This local quantity represents the amount of photons absorbed by the species A per unit of time and per unit of reactor volume. It is expressed as:

$$e^a_{A,\lambda} = \alpha_{A,\lambda} E_\lambda = \kappa_{A,\lambda} C_A E_\lambda \tag{2}$$

where $\alpha_{A,\lambda}$ is the Napierian linear absorption coefficient of the species A (m^{-1}), $\kappa_{A,\lambda}$ the Napierian molar absorption coefficient of the species A (m^2 mol^{-1}), C_A the concentration of the species A (mol m^{-3}) and E_λ the spherical irradiance (mol photon m^{-2} s^{-1}).

The combination of Eqs. (1) and (2) shows that, to determine the mean reaction rate (i.e. averaged over the whole reactor volume), it is necessary to know the concentration fields of the different species (which depend on the hydrodynamics conditions), but also the absorption properties of the medium and the irradiance field. When compared to thermal chemical reactor engineering, a new coupling is thus introduced: the coupling of the radiative transfer equation with other conservation equations, via the photochemical kinetic term.

The first consequence is that, even if the photoreactor is assumed "ideal" from a hydrodynamic point of view (i.e. perfectly mixed or plug flow), a heterogeneous field of the reaction rate exists, due the exponential attenuation of light inside the reactor (Fig. 2). The well-known concept of "ideal reactors" should be then thought again in photochemical reactor engineering.

The other direct consequence is that the occurrence of some gradients of concentrations, due to light attenuation but also to hydrodynamics conditions (mixing), can induce physical limitations, which will slow down the photochemical reaction rate and decrease the performances (productivity, photonic efficiency). To identify these limitations, and thus to elaborate a strategy to overcome or limit them, modelling is an essential tool as it formalizes the coupling between the different phenomena involved.

The introduction of this new coupling significantly increases the degree of complexity of the modelling approach, in particular due to the intrinsic complexity of the radiative transfer equation (integro-differential equation, dependence on spatial and angular coordinates, light emission model, scattering, etc.). As the analytical solutions available in some simplified configurations (in terms of geometry and light emission) cannot be always used, advanced methods, often time-consuming, must be implemented instead, for example the Monte-Carlo method or flux methods (discrete ordinate, two-flux method, etc.) [57–64]. For that, the
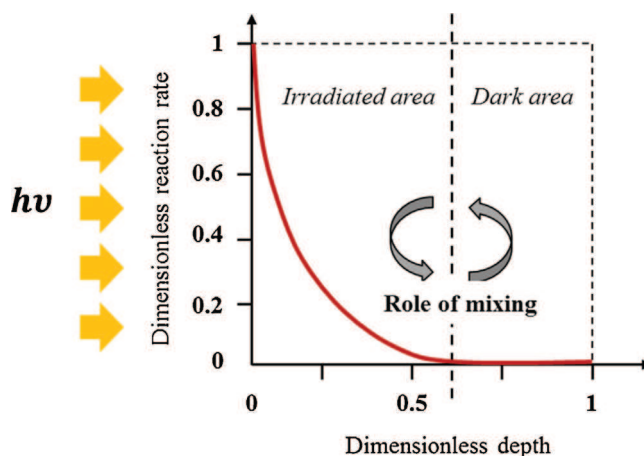

Fig. 2. Light attenuation along the direction of light penetration.

literature on the theory of photoreactor engineering can be used to thoroughly derive reaction engineering principles and radiative energy transport fundamentals [59–71]. The challenges will thus be (i) to bridge the gap between two scientific fields, namely to integrate fundamental principles of radiative transfer and photochemistry into engineering modelling methods, and (ii) to find the most simple and comprehensive models allowing to represent in a sufficiently accurate way all the phenomena involved in a microphotoreactor, and their couplings. This will be illustrated in the following sections.

4. Flow photochemistry: which are the key influencing parameters?

In the following sub-sections, the key parameters influencing the photochemical reaction outputs when carried out in a microstructured technology will be highlighted, based on basic modelling. To illustrate the method, it has been chosen to consider:

- a monochromatic, mono-directional and collimated light source, uniformly distributed along the reactor walls and perpendicularly to the flow direction; the subscript "λ" will be then voluntarily omitted to simplify notations related to all wavelength-dependent physical quantities.
- a straight microreactor which characteristic dimension along the light penetration direction is noted e and the material of the optical surfaces is non-reflective.
- a purely photochemical transformation $A \xrightarrow{h\upsilon} B$ where both the species A and B are absorbing the incident photons at a given wavelength λ; the performances will be then evaluated only in terms of conversion. For more complex reactional schemes, one should also consider selectivity.

4.1. Incident photon flux density and specific irradiated area

Let us consider that the microphotoreactor behaves as a plug-flow reactor. In this case, Aillet et al. [54] showed that, under the assumptions previously reported, a simple equation can be established to describe the variation of the concentration in species A, C_A, with respect to the residence time, τ. For that, a local mass balance is written (an analytical solution for the radiative transfer equation is then considered), followed by an integration over the whole reactor volume. It leads to:

$$-\frac{dC_A}{d\tau} = \Phi \frac{q_p}{V_r} f = \Phi \frac{q_p}{V_r} \frac{\kappa_A C_A}{\kappa_A C_A + \kappa_B C_B} (1 - \exp[-(\kappa_A C_A + \kappa_B C_B)e]) \quad (3)$$

where q_p is the incident photon flux (mol photon s^{-1}), V_r the volume of the microphotoreactor, e the characteristic dimension of the microphotoreactor with respect to the light penetration

direction (path length), κ_A and κ_B the Napierian molar absorption coefficients related to the species A and B, respectively.

In Eq. (3), the factor $\Phi \frac{q_p}{V_r}$ can be seen as a kinetic constant of a zero-order reaction and f is called the photokinetic factor. It is interesting to note that this equation is still valid in a perfectly mixed batch reactor by replacing the residence time by the irradiation time [53,54]. Furthermore, the parameter $\frac{q_p}{V_r}$ can be also expressed as:

$$\frac{q_p}{V_r} = \frac{F_0 \times S_{irrad}}{V_r} = F_0 \times a_{irrad} \quad (4)$$

where F_0 is the photon flux density received at the microphotoreactor's walls (mol photon s^{-1} m^{-2}) and a_{irrad} the specific irradiated area (m^{-1}) defined by the ratio between the irradiated surface, S_{irrad}, and the reactor volume, V_r.
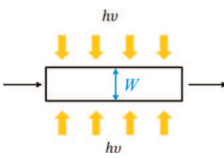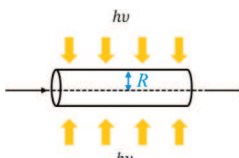
From Eqs. (1), (3) and (4), one can deduce that the maximal average reaction rate (mol m^{-3} s^{-1}) that can be achieved in the microphotoreactor (i.e. if all the incident photons are used by the species A), $\langle r_A \rangle_{max}$, is equal to:

$$\langle r_A \rangle_{max} = \Phi \frac{q_p}{V_r} = \Phi \times F_0 \times a_{irrad} \quad (5)$$

Eq. (5) is fundamental as it highlights that the photochemical reaction rate is directly proportional to the **photon flux density received at walls** and to the **specific irradiated area**. F_0 and a_{irrad} are thus the two levers to intensify a photochemical reaction; they are dependent on both characteristics of the microreactor and of the light source, and also of the way the microreactor is exposed to the light source. Eq. (5) also gives implicitly the main reason explaining why microstructured technologies, combined with the new light sources (like LED), enable enhanced reaction performances when compared to conventional technologies: they offer significantly higher specific irradiated area (few 1000 m^{-1}) and the photon flux densities received at walls are higher and can be adjusted.

Another consequence of Eq. (5) is that the incident photon flux, q_p (i.e. the photon flux really received in the system) should be imperatively known when the objective is to compare results obtained in different (micro)photoreactors or to design a microreactor for a given photochemical reaction. Indeed, considering the photon flux emitted by the light source is not sufficient because only a part of light emitted is really received in the system, mainly due to the non-collimated nature of the light source and/or to the reflectance and transmittance of the microreactor material. With respect to the small dimensions involved in microphotoreactors, direct measurements using a radiometer are not possible; the more efficient alternative is, as proposed by Aillet et al. [55], to implement an actinometry method, which involves a simple photochemical reaction with a known quantum yield.

Table 1
Plug-flow microphotoreactors (irradiated with a monochromatic, mono-directional and collimated light source, uniformly distributed along the reactor walls and perpendicularly to the flow direction): definitions of the characteristic dimension, e, and of the parameter $\frac{q_p}{V_r}$ depending on the geometry.

Parallel plate microreactor irradiated from the outside	Tubular microreactor irradiated from the outside	Annular microreactor irradiated from the inside
$\frac{q_p}{V_r} = \frac{F_0}{W}$ and $e = W$	$\frac{q_p}{V_r} = 2\frac{F_0}{R}$ and $e = 2R$	$\frac{q_p}{V_r} = 2\frac{F_0 R_i}{(R_e^2 - R_i^2)}$ and $e = R_e - R_i$

Finally, it is interesting to note that Eq. (3) can be generalized to three types of geometries of plug-flow microphotoreactors (irradiated with a monochromatic, mono-directional and collimated light source, uniformly distributed along the reactor walls and perpendicularly to the flow direction). These geometries consist in parallel plate microreactors irradiated from the outside, tubular microreactors irradiated from the outside and annular microreactors irradiated from the inside. For that, an ad hoc definition for the characteristic dimension, e, and for $\frac{q_p}{V_r}$ (these two parameters being sufficient to fully characterize ideal microphotoreactors), as shown in Table 1.

4.2. Medium absorbance and competitive absorption factor

Let us define the conversion X as:

$$X = 1 - \frac{C_A}{C_{A0}} \tag{6}$$

Eq. (3) can then be written again as:

$$-\frac{dX}{d\tau} = \Phi \frac{q_p}{V_r C_{A0}} \frac{\beta_A}{(1-X)\beta_A + (1-\beta_A)X} \frac{1-X}{}$$
$$\left(1 - \exp\left[-A_e^0((1-X)\beta_A + (1-\beta_A)X)\right]\right) \tag{7}$$

where C_{A0} is the initial concentration of the species A, β_A the competitive absorbance factor with respect to the species A and A_e^0 a reference absorbance defined as [54]:

$$\beta_A = \frac{\kappa_A}{\kappa_A + \kappa_B} \tag{8}$$

$$A_e^0 = (\kappa_A + \kappa_B)C_{A0} \times e \tag{9}$$

Consequently, Eq. (7) highlights two other important parameters for consideration when carrying out a photochemical reaction in continuous (micro) photoreactors: the **competitive absorbance factor** and the **medium absorbance**.

By definition, β_A gives information on the level of competition between the reactant A and the product B for absorbing the incident photons. To illustrate its influence, an example (deduced from the resolution of Eq. (7)) of the variation of the conversion as a function of residence time for different competitive absorbance factors is presented in Fig. 3a. This figure shows that the more the

product B is absorbing $\beta_A \to 0$), the more the reaction rate is slowed down, the part of photons absorbed by the reagent A being decreasing as far as the conversion increases. This phenomenon, intrinsic to the reaction characteristics, will be more pronounced in the case of non-ideal microphotoreactors for which mass transfer limitations exist (see Section 5.1).

Concerning the medium absorbance, A_e, this parameter changes as far as the reaction progresses, as depending on the conversion X according to:

$$A_e = (\kappa_A C_A + \kappa_B C_B)e = A_e^0 \times [\beta_A(1-X) + X(1-\beta_A)] = A_e^0 \times \beta_A \times \chi$$
$$\text{with } \chi = (1-X) + X\frac{(1-\beta_A)}{\beta_A} \tag{10}$$

where χ is a function of X and of β_A ($\chi = 1$ when $X = 0$, and $\chi = \frac{1-\beta_A}{\beta_A}$ when $X = 1$) and A_e^0 defined in Eq. (9). It is interesting to observe that the medium absorbance can be also seen as a dimensionless number:

$$A_e = \frac{e}{d_{pen}} \tag{11}$$

where d_{pen} is the **characteristic light penetration distance** (also called optical thickness), defined according to

$$d_{pen} = \frac{1}{\kappa_A C_{A0}\chi} \tag{12}$$

As shown by Eq. (11) and Fig. 3b, the light penetration distance decreases when increasing the initial concentration of the species A and the molar absorption coefficient κ_A. If the species B does not absorb ($\beta_A = 1$), d_{pen} will increase as far as the conversion increases (decrease of the function χ): the medium becomes then more and more transparent, whereas, when $\beta_A \leq 0.5$, d_{pen} will decrease and the medium will become more and more opaque. Classically, one considers that $A_e < 1$ corresponds to great optical thickness (i.e. $e < d_{pen}$) and $A_e > 1$ to small optical thickness (i.e. $e > d_{pen}$). In the second case, the fraction between the irradiated and the reactor volumes will be smaller than one, thus implying the appearance of dark zones. In the extreme case, when this fraction tends towards zero, the irradiated volume is located in a narrow zone close to the optical walls, leading to a "surface reaction" or "film reaction". In this case, the role of the mixing (mass transfer) will be crucial to efficiently renew this zone.
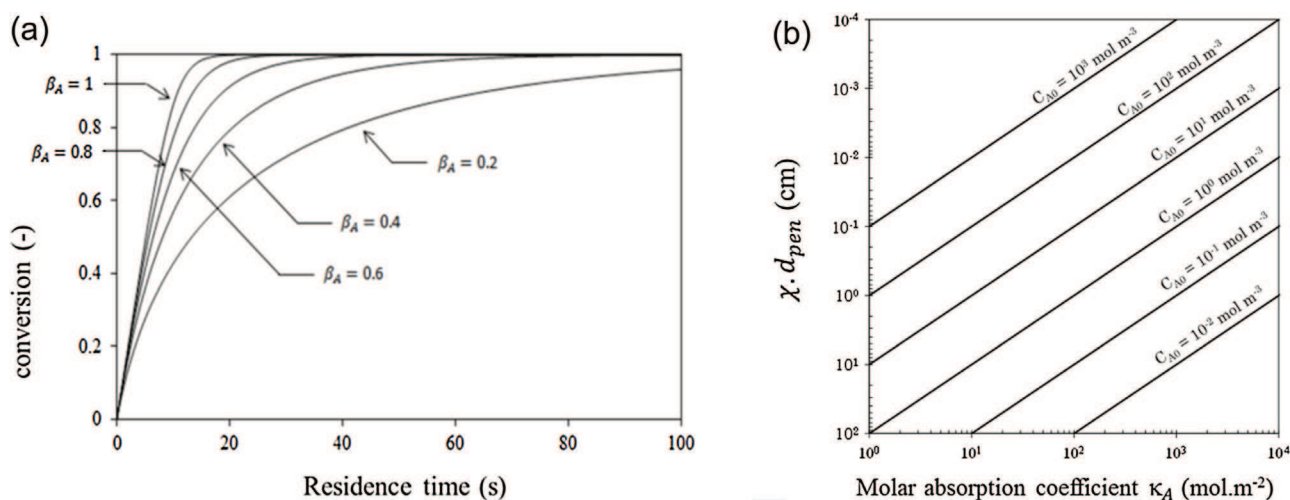
Fig. 3. (a) Variation of the conversion as a function of residence time for different competitive absorbance factor in the case of a plug-flow microphotoreactor ($\Phi\frac{q_p}{V_r} = 10^{-4}$ mol L^{-1} s^{-1}, $\kappa_A = 500$ L mol^{-1} cm^{-1}, $C_{A0} = 0.01$ mol L^{-1}, $e = 1$ cm). (b) Light penetration distance, weighted by the function χ (Eq. 10) as a function of the molar absorption coefficient κ_A and the initial concentration of the species A.

As the molar absorption coefficients of species are intrinsic properties of the reaction, the two levers available to change the medium absorbance are the initial concentration of the species A, C_{A0}, and/or the characteristic dimension of the microreactor, e. Thus, another advantage of microstructured technologies becomes apparent: thanks to their small dimensions, it is possible to work with concentrated media while conserving an acceptable level of absorbance. For the "surface reactions" previously mentioned, falling film microreactors prove to be particularly adapted [51,52].

4.3. Mass transfer limitations

In the previous sub-sections, a plug-flow behavior of the microphotoreactor was assumed to highlight, in a simple way, the key parameters (ϕ, F_0, a_{irrad}, A_e, β_A) influencing the reaction outputs. Unfortunately, such kind of approach is often not sufficient to describe the coupling between all the phenomena inside a microphotoreactor, and in particular the effect of mass-transfer limitations (mixing). To fill this gap, more advanced modelling tools are required. In this perspective, Aillet et al. [54] have proposed a bi-dimensional model enabling to predict the spatial distributions of concentrations and irradiance inside a straight microphotoreactor involving a laminar flow (the radiative transfer equation is solved by the two-flux method [73]). Using a dimensionless set of equations, they showed that the reaction outputs are always controlled by the competitive absorbance factor β_A and the reference medium absorbance A_e^0, but also by two other dimensionless numbers: the **Damköhler I and II numbers**, Da_I and Da_{II}. The latter dimensionless numbers are expressed as the ratio between residence time, τ, and photochemical reaction time, τ_r, and between transverse mixing time, τ_d, and photochemical reaction time, respectively. Considering a photochemical reaction $A \xrightarrow{h\upsilon} B$, a monochromatic collimated light source and a laminar flow inside a straight microreactor irradiated perpendicularly to its width from one or both sides ($\upsilon = 0$ or 1) (parallel plate geometry, see Table 1), they can be expressed as [54]:

$$Da_I = \frac{\tau}{\tau_r} = \frac{\frac{L}{\overline{U}}}{\frac{C_{A0}e}{\Phi(1+\upsilon)\beta_A F_0}} \tag{13}$$

$$Da_{II} = \frac{\tau_d}{\tau_r} = \frac{\frac{e^2}{D_m}}{\frac{C_{A0}e}{\Phi(1+\upsilon)\beta_A F_0}} \tag{14}$$

where $\overline{U}$ is the mean velocity in the microreactor, L and e the length (along the axial direction) and the transverse dimension (along the light penetration direction) of the microphotoreactor and D_m the diffusion coefficient.

These two dimensionless numbers are common in chemical engineering, but their transposition to photochemical reactions is not direct as it implies to correctly define the characteristic reaction time. Contrary to thermal reactions, for which some intrinsic kinetics laws are formulated, the characteristic time of the photochemical reaction is process-dependent (i.e. no more intrinsic to the reaction system) because the reaction rate, r, depends on the volumetric rate of photon absorption, e^a (Eq. (1)) and thus on the irradiance, E (Eq. (2)). Its definition should then be adapted, for each reaction, but also for each light source/micro-reactor technology. The characteristic time reported in Eqs. (13) and (14) was deduced, for strongly absorbing media, from the average of the local reaction times over a conversion varying between 0 and 1, and not from the reaction rate at the beginning of the reaction when the conversion is null, as it is classically done for thermal reactions; such method enables to take into account the effect of β_A on the reaction time [54].

The Damköhler I number can be regarded as a measure of the conversion that can be achieved: high values of Da_I mean complete conversions at the microreactor outlet. It is interesting to note that Da_I is also directly linked to the dose, that is, to the amount of photons received during the residence time per unit of reactor volume (mol photon m^{-3}), defined as:

$$\text{dose} = \frac{q_p}{V_r}\tau \tag{15}$$

thus implying:

$$Da_I = \text{dose}\frac{\Phi}{C_{A0}}\beta_A \tag{16}$$

The Damköhler II number can be regarded as a measure of the efficiency of the mixing (or mass transfer) along the optical light path, which is induced, in Eq. (14), by molecular diffusion. The latter represents one of the two main phenomena responsible for the occurrence of concentration gradients in the transverse direction, namely the light attenuation (the other one being the heterogeneous velocity field along the transverse direction due to the laminar flow). A value of Da_{II} smaller than one means that the transverse mass transfer time is shorter than the characteristic time of the reaction. Another advantage of microstructured technologies can be pointed out here: due to their small scales, the transverse mass transfer times are significantly reduced, which enables to overcome this type of limitations commonly encountered in conventional photochemical equipment and thus to improve reaction outputs and/or to carry out reactions under safer conditions.

Naturally, both Damköhler numbers are linked via the Fourier number, Fo, as:

$$Da_{II} = \frac{1}{Fo}Da_I \tag{17}$$

From Eq. (17), a diagram can be established to identify the different zones in which a microphotoreactor can operate, as shown by Aillet et al. [54]. The "optimal" domain avoiding mass transfer limitations (no concentration gradients along the transverse direction, plug-flow behavior) corresponds to the cases where $Da_{II} < 1$ and $1/Fo < 1$.

It is important to note that, even if some strategies can be elaborated to avoid mass-transfer limitations (see Section 5.1), this presupposes indirectly that the lifetime of electronically excited species is long enough to enable the reaction to occur. If this is not the case, mixing will be no longer the limiting parameter and other strategies (a change of solvent for example) will have to be implemented to increase the lifetime of the excited species.

When more complex geometries of microphotoreactors (meandering channels for example) are involved or when heterogeneous reactions are carried out, it will be necessary to adapt or complete this analysis based on the dimensionless numbers. Mass transfer coefficients should be in particular considered.

4.4. Productivity and photonic efficiency

From a chemical engineering point of view, the performances obtained in a given microphotoreactor can be generally evaluated through both productivity and photonic efficiency.

The **productivity**, R^X, is defined for a given conversion X, as:
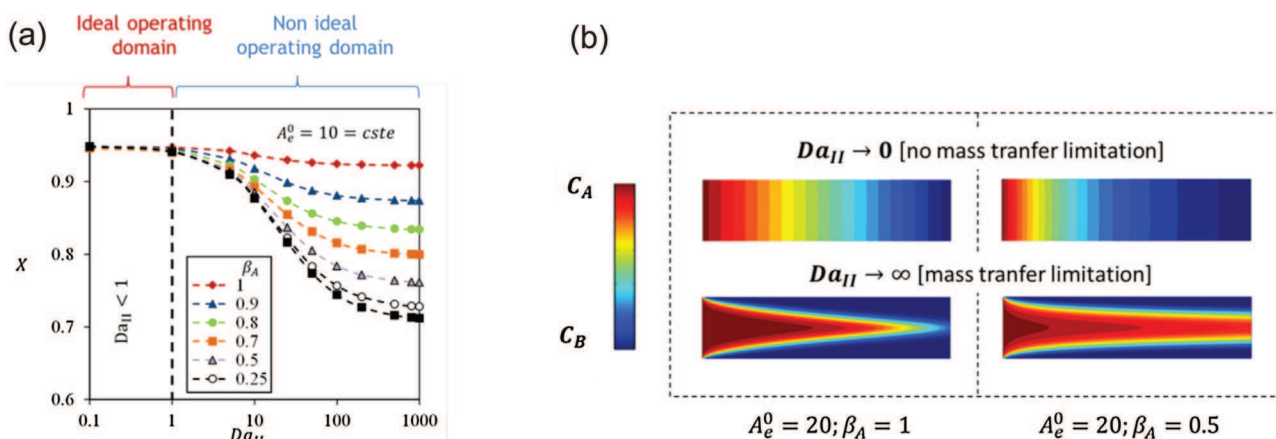
$$R^X = \frac{n}{\tau_X} \tag{17}$$

Fig. 4. Effect of mixing limitations: (a) Conversion at the outlet of the microreactor versus Damköhler II number for different competitive absorbance factors ($A_e^0 = 10$). (b) Concentration fields inside the microphotoreactor for two limit cases ($Da_{II} \to 0$ and $Da_{II} \to \infty$), depending on the competitive absorption factor β_A ($A_e^0 = 20$).

where n is the number of moles of product formed and τ_X the residence time necessary to reach a given conversion X. According to Eq. (3), this residence time is inversely proportional to n/q_p. Consequently, the productivity is proportional to the incident photon flux, q_p, and using Eq. (4), one finds:

$$R^X \propto q_p \text{ leading to } R^X \propto F_0 \times a_{irrad} \times V_r \qquad (18)$$

In a process intensification strategy, Eq. (18) has important consequences as it implies that an increase in productivity necessarily requires an increase in q_p. For that, several choices are available: increasing the photon flux density at the reactor walls (F_0) and/or the irradiated specific area (a_{irrad}) and/or the reactor volume (V_r). In this perspective, photochemical equipment based on the concept of plate heat-exchangers are particularly interesting, as they allow to maintain, for each fluidic module in series, identical F_0 and a_{irrad} thanks to LED arrays placed on both sides of each fluidic module. Consequently, the productivity can be simply increased by raising the reactor volume, namely by multiplying the number of fluidic module in series (see Ref. [47]).

Nevertheless, one should keep in mind that the productivity is not only controlled by the incident photon flux, but also by the absorbance properties of the medium (if the absorbance is low, few photons will be absorbed and the productivity will be low). For this reason, one should introduce another criteria: the *photonic*

efficiency, η^X. It is defined, for a given conversion X, as the ratio between the number of moles of reactant converted (or product formed) and the number of photons received in the microreactor, corrected by the quantum yield [53]:

$$\eta^X = \frac{n}{\phi \times q_p \times \tau_X} \qquad (19)$$

It evaluates the optimal use of photons in the microreactor. Indeed, as quantified by the quantum yield (see Section 3), not all of the photons absorbed necessarily lead to the conversion of the compound A. However, other phenomena can increase the number of photons required to form the product B:

- the hydrodynamics inside the microreactor. For example, when the product B or other species absorb the incident photons, poor mixing conditions can generate an overexposure of these molecules to the detriment of the reactant A, and thus reduce the part of photons available for A (see Section 5.1),
- the medium absorbance. If the medium absorbance is low, a significant part of the photons are transmitted over the back optical walls if this latter is transparent (no reflector).

The photonic efficiency enables the two latter phenomena to be taken into account. It is corrected by the quantum yield to free it
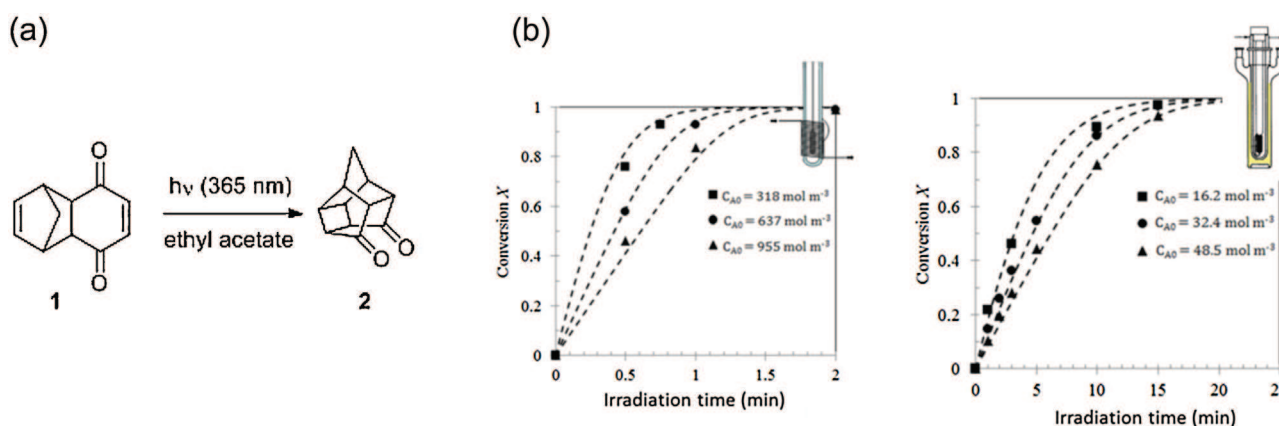

Fig. 5. Predictions of the performances obtained: (a) synthesis of a pentacyclic cage compound [47,53], (b) conversion versus irradiation time in a capillary tower microreactor and in an immersion well reactor (dotted lines: predicted values by Eq. (20)).

from the effect of deactivation processes intrinsic to the photochemical reaction mechanisms. Ideally, it should tend to 1 (one mole of photons used to form one mole of product).

From Eqs. (17) and (19), the productivity and the photonic efficiency are closely linked [54] according to:

$$R^X = \phi \times q_p \times \eta^X = \phi \times F_0 \times a_{irrad} \times V_r \times \eta^X \qquad (20)$$

Eq. (20) confirms that, to maintain a constant productivity between two plug-flow (micro)reactors, one should conserve both incident photon flux $\left(q_p\right)$ and photonic efficiency (η^X). Eq. (20) also shows that, if the intrinsic parameters of the reaction are known (quantum yield, molar absorption coefficients), one can determine the requirements in terms of incident photon flux density (design of the light source), of irradiated specific area and reactor volume (design of the microreactor and integration of the light source around it), and of photonic efficiency (medium absorbance) in order to reach a given productivity in plug-flow (micro) reactors.

5. Illustrative examples

This part will present some illustrative examples extracted from our previous studies. In all these examples, purely direct photochemical reactions $A \xrightarrow{h\upsilon} B$ occurring in homogenous medium are considered. The objective is to demonstrate how a chemical engineering framework, such as presented in the previous sections, enables to understand the coupling between the different phenomena involved (Section 5.1), to predict the performances obtained (Section 5.2), to acquire kinetics data on a photochemical reaction (Section 5.3) or to elaborate a strategy for photochemical process intensification (Section 5.4).

5.1. Understanding the coupling between the different phenomena involved

As mentioned in the previous section, the mixing along the light penetration depth can have an influence of the reaction outputs. This phenomenon has been highlighted, numerically and experimentally, by Aillet et al. [54] and Aillet et al. [74] respectively, in the case of a photochemical reaction $A \xrightarrow{h\upsilon} B$. For illustrative purpose, Fig. 4a reports, for a strong absorbing medium $\left(A_e^0 = 10\right)$, numerical results describing the conversion at the microreactor

outlet, X, as a function of the Damköhler II number, Da_{II} (Eq. (14)) and of the competitive absorbance factors, β_A. One can observe that a significant decrease in conversion exists when increasing Da_{II}, namely when the transverse mixing becomes slower and slower. The smallest the competitive absorption factor is β_A (i.e. the highest the molar absorption coefficient of the product B, κ_B), the more pronounced the effect of Da_{II} is.

To physically understand such trends, the corresponding concentration fields in the microphotoreactor should be analyzed (Fig. 4b). When the product B absorbs at the same wavelength than the reactant A $(\beta_A < 1)$ and when the medium is strongly absorbing $\left(A_e^0 = 10\right)$, strong concentration gradients appear as far as Da_{II} increases. This is directly due to the formation, from the initial moments of the reaction, of a layer of product B close to the microreactor wall where the light is the most intense. This layer plays the role of a screen or a filter, which prevents the photon to penetrate further inside the microreactor and to react with the reactant A. It persists throughout the microreactor length as the mixing (mass transfer by diffusion) does not enable the fluid at the wall to be efficiently renewed. Another way to evaluate this phenomenon is to numerically calculate the average volumetric rates of photons absorbed by the compounds A and B in the microreactor, $\left\langle e_A^a \right\rangle$ and $\left\langle e_B^a \right\rangle$ [54]. One can then observe that the amount of photons absorbed by the compound B increases when increasing Da_{II}. In practise, special attention should be paid to this fact because, in the case of light-sensitive products, some photodecomposition may occur and may thus impact on the reaction selectivity.

Aillet et al. [54] have identified two particular cases for which the occurrence of mass transfer limitations $(Da_{II} > 1)$ has a negligible influence on the conversion:

- When the species A is the single absorbing species $(\beta_A = 1)$. In this case, the absorbing layer shifts to the center of the microreactor as far as the conversion progresses (see Fig. 4b), thus meaning that the medium becomes more and more transparent.
- When the medium absorbance is low $\left(A_e^0 < 5\right)$. The microreactor is then fully illuminated.

In both cases, the transverse mixing slightly impacts the conversion because the molecules of reactant A do not need to
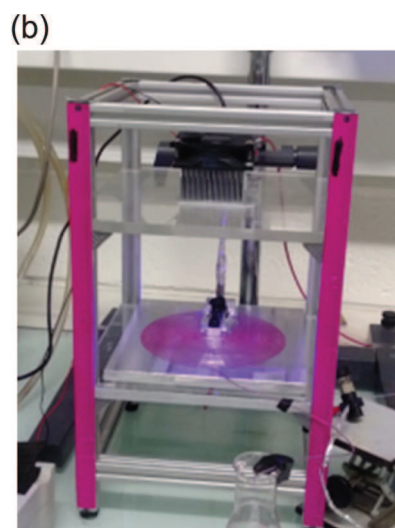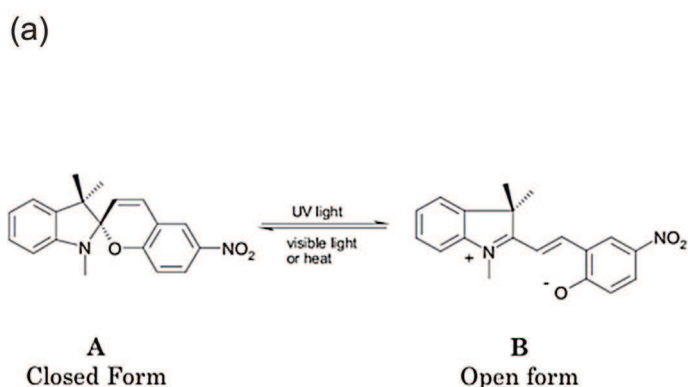

Fig. 6. Acquisition of kinetic data: (a) reversible reaction between the closed and the open forms of TMINBPS [56], (b) spiral-shaped microreactor irradiated by a LED array.

travel efficiently along the light penetration direction as the photons can penetrate inside the medium to reach the non-excited molecules. For microreactor modelling, this is an optimal situation as it implies that the microreactor can be considered as a plug-flow reactor.

5.2. Predicting the performances obtained

The synthesis of a pentacyclic cage compound (Fig. 5a) was carried out by Aillet et al. [53] in a classical immersion well reactor ($V_r = 225$ mL, $e = 0.62$ cm) and a capillary-tower microreactor ($V_r = 0.81$ mL, $e = 0.0508$ cm), both irradiated by a medium pressure mercury lamp. It was observed that full conversions were achieved within a few minutes of residence times in the microreactor whereas irradiation times longer than 20 min were required in the batch reactor (Fig. 5b). As the cage compound does not absorb the incident photons at 365 nm ($\beta_A = 1$), the following analytical solution for t_{irrad} could be obtained from Eq. (7):

$$t_{irrad} = \frac{V_r C_{A0}}{q_p\,\Phi}\left(X + \frac{1}{A_e^0}\ln\left[\frac{1 - \exp\left(-A_e^0\right)}{1 - \exp\left(-A_e^0(1 - X)\right)}\right]\right) \quad (20)$$

which can be also written, using Eq. (13) and considering $\tau = t_{irrad}$, as

$$Da_I = \text{dose}.\frac{\Phi}{C_{A0}} = \left(X + \frac{1}{A_e^0}\ln\left[\frac{1 - \exp\left(-A_e^0\right)}{1 - \exp\left(-A_e^0(1 - X)\right)}\right]\right) \quad (21)$$

As shown in Fig. 5b, the experimental variations of the conversion, X, as a function of the irradiation time, t_{irrad}, are successfully predicted by Eq. (20) in both reactors. Such good agreement validates that, when $\beta_A = 1$, the batch reactor can be described as a perfectly mixed reactor and the microreactor as a plug-flow reactor (see Section 5.1).

It is also interesting to use Eq. (20) as a mean to understand why the irradiation times are so different in both reactors. Indeed, the irradiation time ratio, χ_t^X, required to reach a conversion X, for example equal to 90%, at a given absorbance A_e^0, can be calculated as:

$$\chi_t^X = \frac{(t_{irrad})_{batch}}{(t_{irrad})_{micro}} = \frac{\left(q_p/V_r\right)_{micro}}{\left(q_p/V_r\right)_{batch}} \times \frac{(C_{AO})_{batch}}{(C_{AO})_{micro}}$$
$$= \frac{(a_{irrad} \times F_0)_{micro}}{(a_{irrad} \times F_0)_{batch}} \times \frac{(C_{AO})_{batch}}{(C_{AO})_{micro}} \quad (22)$$

Using the data reported in Ref. [53] and the results obtained by actinometry [55], an irradiation time ratio close to 17 is obtained, which is in perfect agreement with the experimental ratio (Fig. 5b). An in-depth analysis reveals that such a result is due to a difference in terms of initial concentrations (A_e^0 is constant in both reactors), but also in terms of irradiated specific area (2530 m^{-1} in microreactor against 133 m^{-1} in batch reactor) and of incident photon flux density (2.55×10^{-3} mol photon m^{-2} s^{-1} in microreactor against 0.23×10^{-3} mol photon m^{-2} s^{-1} in batch reactor).

The relevancy of this modelling approach (Eq. (20)) has also been demonstrated when this reaction was carried out in the meso-scale continuous reactor commercialized by Corning (Corning® Advanced-Flow™ G1 photo reactor), either composed by one or five fluidic modules, as recently illustrated by Elgue et al. [47].

5.3. Acquiring kinetic data

Recently, microreactors were used, for the first time, as a tool for acquiring kinetic data on a photochemical reaction [56]. For illustration purpose, a thermal photochromic system (1,3,3-trimethylindolino-6′-nitrobenzopyrylospiran, named TMINBPS) was chosen (Fig. 6a). It involves a reversible system where the initial colorless species (closed form) reacts photochemically via a step characterized by the quantum yield Φ_{AB}. The species formed (open form with a pink color) has a short lifetime and is transformed into A by a thermal reaction characterized by a rate k_t. The two kinetics parameters of the reaction (Φ_{AB}, k_t) were successfully determined by combining modelling tools (such as described in Sections 4.1 and 4.2) and specific experiments in a spiral-shaped microreactor irradiated by a UV-LED array (Fig. 6b). For that, the incident photon flux, q_p, should be imperatively known; actinometry measurements were thus carried out, according to the protocol defined by[55].

This work [56] offers promising perspectives for a new usage of microreactors for photochemistry. Indeed, the ability to use microreactors for acquiring kinetic data of a photochemical reaction is an undeniable advantage, and all the more that this can be done rapidly, with low volumes handled and in an experimental window enlarged to operating conditions inaccessible for batch reactors (short residence time, high concentration). This is particularly interesting in a process intensification strategy where an in-depth knowledge of reaction kinetic will ensure reliability in extrapolation and in process modeling.
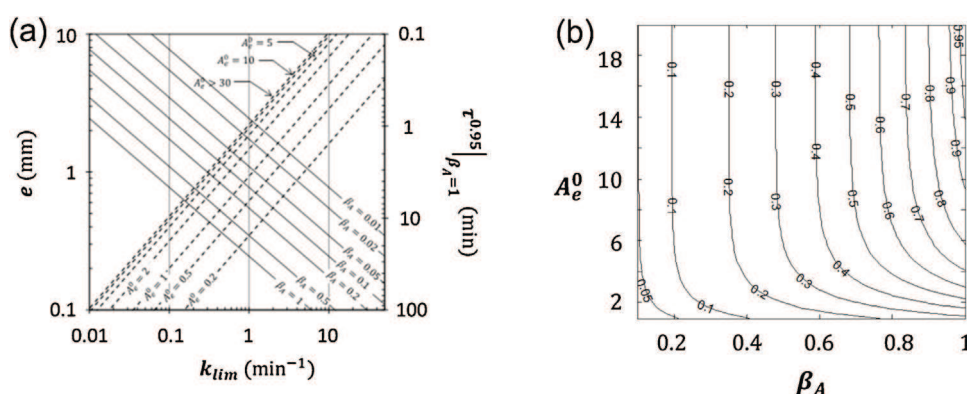

Fig. 7. Elaboration of strategies for photochemical process intensification: (a) diagram for determining the maximal photon flux density and the minimal residence time to avoid mass transfer limitations in microreactor. (b) no mass transfer limitations: Iso-curves for photonic efficiency (for a conversion of 95%) as a function of the dimensionless numbers A_e^0 and β_A.

5.4. Elaborating strategies for photochemical process intensification

Using the modelling background presented in Section 4, strategies can be built to determine the optimal conditions in which a microreactor should operate or to address scale-up issues. In the following, some examples will be presented, always in the case of a photochemical transformation $A \overset{h\upsilon}{\rightarrow} B$.

The occurrence of mass transfer limitations (slow mixing along the light penetration direction) can induce a significant decrease of the conversion at the outlet of the microreactor (see Fig. 4a), but also on the productivity via the decrease of the photonic efficiency (see [54]). Starting from these findings, several strategies can be devised for maximizing the productivity in microreactors. One of them is to identify the conditions under which the micro-photoreactor behaves as a plug-flow reactor (homogeneous concentration profiles in the transverse direction). For that, according to Section 4.3, the Damköhler II number, Da_{II}, should be kept below 1 while conserving also the inverse of the Fourier number, $1/Fo$, below 1. Eq. (14) shows that one can act on two levers to fill these conditions: the characteristic dimension of the microphotoreactor in the transverse direction, e, and the incident photon flux density, F_0. In this perspective, a diagram (built from numerical results) has been proposed by Aillet et al. [54], enabling to determine, for a given characteristic dimension, e, and depending on the medium absorbance, A_e^0 and competitive absorption factor, β_A (associated with a photochemical reaction $A \overset{h\upsilon}{\rightarrow} B$), the conditions in which the microreactor should operate to achieve a high conversion (for example 95%) while avoiding mass transfer limitations (Fig. 7a). More particularly, these conditions correspond to:

- a maximal photon flux density, $F_{0,max}$, to impose. Indeed, as predicted by Eq. (14), the reaction characteristic time, τ_r is inversely proportional to F_0; consequently, defining a maximal value for F_0 enables to ensure that the transverse mixing time, τ_d, remains smaller than τ_r; in Fig. 7a, $F_{0,max}$ is deduced from the coefficient k_{lim} reported on the abscissa axis (see Ref. [54] for details),
- a minimal residence time (τ_{min}) to impose, which is linked to the previous maximal photon flux density. It is deduced from the residence time required to reach a conversion of 95% in the case where $\beta_A = 1$ (noted $\tau^{0.95}|_{\beta_A=1}$) which is reported on the right-side ordinate axis of Fig. 7b. The value of $\tau^{0.95}|_{\beta_A=1}$ read on the diagram should be then multiplied by the function $H^{0.95}\left(\beta_A, A_e^0\right)$ defined in Ref. [54] to account for the effect of the medium absorbance and competitive absorption factor.

Such a diagram can be also used as a tool for quantifying the effect of the miniaturization of the microreactor on the productivity, R^X, in the case where no mass transfer limitations exist [54]. For that, $F_{0,max}$ and τ_{min} associated with different microreactor dimensions, e, have to be determined and then, from the knowledge of $\left(\beta_A, A_e^0\right)$ and of the photonic efficiency (Fig. 7b), R^X can be deduced for each [54].

Once having determined the conditions $\left(F_{0,max}, \tau_{min}\right)$ with respect to avoiding mass transfer limitations in a given micro-reactor, or when these limitations have a negligible influence (see Section 5.1), a new diagram can be constructed (from Eqs. (7) and (13)) reporting the variation of the Damköhler I number, Da_I, required to reach a given conversion, X, as a function of the

reference absorbance, A_e^0, and of the competitive absorbance factor, β_A. Such a diagram, detailed in Ref. [54], reveals that, for strongly absorbing media $\left(A_e^0 > 5\right)$, the Damköhler I number, Da_I, required to reach a given conversion, X, becomes independent on the absorbance, and depends only of β_A, as:

$$Da_I = dose \times \frac{\Phi}{C_{A0}} = -(1 - \beta_A)(X + \ln(1 - X)) + \beta_A X \qquad (24)$$

The latter equation gives two important guidelines:

- when the product B absorbs the incident photons ($\beta_A < 1$), the value of Da_I (and thus of the dose) required to reach a given conversion, X, should be increased to counterbalance the fact that a part of the incident photons is absorbed by the product B.
- an easy method to calculate the dose required to reach a given conversion.

In a smart scale perspective (e.g. from lab-scale microreactors producing few $\mu g\,h^{-1}$ or $mg\,h^{-1}$ to meso-scale continuous reactors producing few $kg\,h^{-1}$), the latter information means that, to maintain the same conversion at both scales when $A_e^0 > 5$, one should conserve a single criteria: the dose; this can be achieved by adapting the residence time and/or the incident photon flux (Eq. (15)). Nevertheless, one should keep in mind that the dose alone does not allow to fully design a continuous (micro) reactor; the productivity, R^X, also has to be considered, which depends on the photonic efficiency, η^X (Eq. (20)). As shown in Fig. 7b, when no mass transfer limitations exist (or when their influence are negligible), the more the medium is absorbing and the less the species B is absorbing, the higher the photonic efficiency η^X is. This shows that working with low absorbances is not a priori optimal firstly because diluted medium implies higher solvent needs and thus heavier downstream processes, but also in terms of energetic efficiency as a part of photons is wasted by transmittance if no reflector is used. Nevertheless, in practice, when mass transfer limitations cannot be overcome (for example, when the light source emitted by the lamp cannot be modified), the usage of low absorbances can be a means to limit their impact on the reaction outputs (conversion, productivity and photonic efficiency); an optimum for the absorbance has then to be found [54].

To conclude, the understanding and the modeling of the phenomena involved (and of their coupling) are absolutely required to determine the optimal operation domain in which a given microphotoreactor should operate to maximize reactions outputs and also to help the design process. Nevertheless, in a photochemical process intensification perspective, it is only a global process analysis (as proposed by Loponov et al. [29]) that will enable to decide if microstructured technologies operate more profitable than other photoreactor technologies. The cost function ultimately will be the deciding factor and its optimization will be used to reveal the true interactions between different competing factors in a complex industrial system (the findings obtained will strongly depend on the photochemical reaction considered). In addition, it is important to remember that, even if their use for production purpose are not always profitable, microstructured technologies remain a powerful tool at laboratory-scale for synthetizing a few milligrams of a product used afterwards in early research and development, and also for investigating photochemical reactions (operating condition screening, kinetic data acquisition, see Section 5.3).

6. Conclusion

Continuous-flow photochemistry is the subject of a growing amount of research and industrial projects as microstructured reactors provide new scientific and technological solutions to optimize photochemical reaction protocols and to overcome problems encountered in conventional photochemical equipment. This present paper illustrates that some of the current challenges and issues in continuous-flow photochemistry can be addressed within a chemical engineering framework. Based on a basic modelling approach and by considering only the case of purely direct photochemical reactions $A \xrightarrow{h\nu} B$ occurring in homogenous medium, the key factors to consider when implementing such photochemical reactions in microstructured technologies were outlined, namely the photon flux density received at walls, the irradiated specific area, the medium absorbance, the competitive absorbance factor and the influence of the mixing along the light penetration direction. Their influence on the reaction outputs (conversion, productivity, photonic efficiency) was analyzed in detail. The interest of this framework was at last demonstrated, for these types of photochemical reactions, using several illustrative examples extracted from our previous studies; they concerned the understanding of the coupling between the different phenomena involved, the predictions of the performances obtained, the acquisition of kinetics data, and the elaboration of strategies for photochemical process intensification.

In the future, the challenge will be to integrate the complexity of photochemistry (e.g. heterogeneous phase reactions, indirect scheme, competitive or consecutive photoreactions) into the present modelling tools so as to enlarge the spectrum of photochemical process intensification strategies. To succeed, two conditions will be required:

- using the current literature on the theory of photoreactor engineering in order to rigorously derive reaction engineering principles and radiative energy transport fundamentals.
- closely interconnecting photochemistry and chemical engineering from the beginning of a study in order to identify reaction and process limitations as soon as possible, and to develop a strategy to overcome these.

References

[1] C.-L. Ciana, C.G. Bochet, Clean and easy photochemistry, Chimia 61 (2007) 650–654.

[2] N. Hoffmann, H. Bouas-Laurent, J.-C. Gramain, Synthèse par voie photochimique, Actualité Chimique 317 (2008) 6–11.

[3] N. Hoffmann, Photochemical reactions as key steps in organic synthesis, Chem. Rev. 108 (2008) 1052–1103.

[4] T. Bach, J.P. Hehn, Photochemische Reaktionen als Schlüsselschritte in der Naturstoffsynthese, Angew. Chem. 123 (2011) 1032–1077.

[5] H.E. Zimmerman, Mechanistic organic photochemistry, Angew. Chem. Int. Ed. 8 (1) (1969) 1–88.

[6] N.J. Turro, Geometric and topological thinking in organic chemistry, Angew. Chem. Int. Ed. 25 (10) (1986) 882–901.

[7] M. Olivucci, F. Santoro, Chemical selectivity through control of excited-state dynamics, Angew. Chem. Int. Ed. 47 (2008) 6322–6325.

[8] I. Schapiro, F. Melaccio, E.N. Laricheva, M. Olivucci, Using the computer to understand the chemistry of conical intersections, Photochem. Photobiol. Sci. 10 (2011) 867–886.

[9] N. Hoffmann, Photochemical reactions of aromatic compounds and the concept of the photon as a traceless reactant, Photochem. Photobiol. Sci. 11 (11) (2012) 1613–1641.

[10] M. Oelgemöller, Green photochemical processes and technologies for research & development, scale-up and chemical production, J. Chin. Chem. Soc. 61 (2014) 743–748.

[11] S. Protti, D. Dondi, M. Fagnoni, A. Albini, Photochemistry in synthesis: where, when, and why, Pure Appl. Chem. 79 (2007) 1929–1938.

[12] P.T. Anastas, M.M. Kirchhoff, Origins, current status, and future challenges of green chemistry, Acc. Chem. Res. 35 (9) (2002) 686–694.

[13] P. Anastas, N. Eghbali, Green chemistry: principles and practice, Chem. Soc. Rev. 39 (2010) 301–312.

[14] H. Baumann, U. Ernst, M. Goez, A. Griesbeck, M. Oelgemöller, T. Oppenländer, M. Schlörholz, B. Strehmel, Licht als kleinstes Reagenz und Werkzeug, Nachr. Chem. 62 (2014) 507–512.

[15] A. Griesbeck, H. Ihmels, K. Licha, T. Mielke, M. Senge, B. Strehmel, D. Wöll, Licht für Medizin und Diagnostik, Nachr. Chem. 62 (2014) 612–616.

[16] J. Iriondo-Alberdi, M.F. Greaney, Photocycloaddition in natural product synthesis, J. Eur. J. Org. Chem. (2007) 4801–4815.

[17] K. Matsuda, M. Irie, Diarylethene as a photoswitching unit, J. Photochem. Photobiol. C: Photochem. Rev. 5 (2004) 169–182.

[18] G.S. Kottas, L.I. Clarke, D. Horinek, J. Michl, Artificial molecular rotors, Chem. Rev. 105 (2005) 1281–1376.

[19] K. Szaciłowski, W. Macyk, A. Drzewiecka-Matuszek, M. Brindell, G. Stochel, Bioinorganic photochemistry: frontiers and mechanisms, Chem. Rev. 105 (2005) 2647–2694.

[20] R. de Richter, S. Caillol, Fighting global warming: the potential of photocatalysis against CO_2, CH_4, N_2O, CFCs, tropospheric O_3, BC and other major contributors to climate change, J. Photochem. Photobiol. C: Photochem. Rev. 12 (2011) 1–19.

[21] M. Tahir, N.S. Amin, Recycling of carbon dioxide to renewable fuels by photocatalysis: prospects and challenges, Renew. Sustain. Energy Rev. 25 (2013) 560–579.

[22] M.R. Hoffmann, S.T. Martin, W. Choi, D.W. Bahnemann, Environmental applications of semiconductor photocatalysis, Chem. Rev. 95 (1995) 69–96.

[23] A.M. Bugaj, Targeted photodynamic therapy—a promising strategy of tumor treatment, Photochem. Photobiol. Sci. 10 (2011) 1097–1109.

[24] K.F. Jensen, B.J. Reizman, S.G. Newman, Tools for chemical synthesis in microsystems, Lab Chip 14 (2014) 3206–3212.

[25] E.E. Coyle, M. Oelgemöller, Micro-photochemistry: photochemistry in microstructured reactors. The new photochemistry of the future? Photochem. Photobiol. Sci. 7 (2008) 1313–1322.

[26] M. Oelgemöller, O. Shvydkiv, Recent advances in microflow photochemistry, Molecules 16 (2011) 7522–7550.

[27] J.P. Knowles, L.D. Elliot, K.I. Booker-Milburn, Flow photochemistry: old light through new windows, Beilstein J. Org. Chem. 8 (2012) 2025–2052.

[28] Y. Su, N.J.W. Straathof, V. Hessel, T. Noël, Photochemical transformations accelerated in continuous-flow reactors: basic concepts and applications, Chem. Eur. J. 20 (34) (2014) 10562–10589.

[29] K.N. Loponov, J. Lopez, M. Barlog, E.V. Astrova, A.V. Malkov, A.A. Lapkin, Optimization of a scalable photochemical reactor for reactions with singlet oxygen, Org. Proc. Res. Dev. 18 (11) (2014) 1443–1454.

[30] D. Ziegenbalg, B. Wriedt, G. Kreisel, D. Kralisch, Investigation of photon fluxes within microstructured photoreactors revealing great optimization potentials, Chem. Eng. Technol. 39 (1) (2016) 1–13.

[31] Y. Su, K. Kuijpers, V. Hessel, T. Noel, A convenient numbering-up strategy for the scale-up of gas–liquid photoredox catalysis in flow, React. Chem. Eng. (2016), doi:http://dx.doi.org/10.1039/c5re00021a.

[32] K.-H. Pfoertner, T. Oppenlander, Photochemistry, Ullmann's Encyclopedia of Industrial Chemistry, Wiley-VCH Verlag GmbH & Co. KGaA, Weinheim, Germany, 2000.

[33] A.M. Braun, M.-T. Maurette, E. Oliveros, Technologie Photochimique, Presses Polytechniques Romandes, 1986.

[34] A.M. Braun, G.H. Peschl, E. Oliveros, Industrial photochemistry, in: A. Griesbeck, M. Oelgemöller, F. Ghetti (Eds.), CRC Handbook of Organic Photochemistry and Photobiology, CRC Press, 2012, pp. 1–19.

[35] M. Fischer, Industrial applications of photochemical syntheses, Angew. Chem. Int. Ed. Engl. 17 (1978) 16–26.

[36] M.C. DeRosa, R.J. Crutchley, Photosensitized singlet oxygen and its applications, Coord. Chem. Rev. 233–234 (2002) 351–371.

[37] T.J. Turconi, F. Griolet, R. Guevel, G. Oddon, R. Villa, A. Geatti, M. Hvala, K. Rossen, R. Göller, A. Burgard, Semisynthetic artemisinin, the chemical path to industrial production, Org. Process Res. Dev. 18 (2014) 417–422.

[38] W.-K. Jo, R.J. Tayade, New generation energy-efficient light source for photocatalysis: LEDs for environmental applications, Ind. Eng. Chem. Res. 53 (2014) 2073–2084.

[39] K. Terao, Y. Nishiyama, S. Aida, H. Tanimoto, T. Morimoto, K. Kakiuchi, Diastereodifferentiating [2 + 2] photocycloaddition of chiral cyclohexenone carboxylates with cyclopentene by a microreactor, J. Photochem. Photobiol. A: Chem. 242 (2012) 13–19.

[40] O. Shvydkiv, S. Gallagher, K. Nolan, M. Oelgemöller, From conventional to micro-photochemistry: photodecarboxylation reactions involving phthalimides, Org. Lett. 12 (2010) 5170–5173.

[41] M. Nettekoven, B. Püllmann, R.E. Martin, D. Wechsler, Evaluation of a flow-photochemistry platform for the synthesis of compact modules, Tetrahedron Lett. 53 (2012) 1363–1366.

[42] S.A.M.W. van den Broek, R. Becker, K. Koch, P.J. Nieuwland, Microreactor technology: real-time flow measurements in organic synthesis, Micromachines 3 (2012) 244–254.

[43] A. Vasudevan, C. Villamil, J. Trumball, J. Olson, D. Sutherland, J. Pan, S. Djuric, LOPHTOR: a convenient flow-based photochemical reactor, Tetrahedron Lett. 51 (2010) 4007–4009.

[44] B.G. Anderson, W.E. Bauta, W.R. Cantrell, Development of an improved process for doxercalciferol via a continuous photochemical reaction, Org. Process Res. Dev. 16 (2012) 967–975.

[45] T. Horie, M. Sumino, T. Tanaka, Y. Matsushita, T. Ichimura, J.-I. Yoshida, Photodimerization of maleic anhydride in a microreactor without clogging, Org. Process Res. Dev. 14 (2010) 405–410.

[46] S. Josland, S. Mumtaz, M. Oelgemöller, Photodecarboxylations in an advanced meso-scale continuous flow photoreactor, Chem. Eng. Technol. 39 (1) (2016) 81–87.

[47] S. Elgue, T. Aillet, K. Loubière, A.-L. Conté, O. Dechy-Cabaret, L. Prat, R. Chemens, O. Horn, S. Vallon, Flow photochemistry: a meso-scale reactor for industrial applications, Chem. Todays 33 (5) (2015) 42–44.

[48] M. Oelgemöller, Highlights of photochemical reactions in microflow reactors, Chem. Eng. Technol. 35 (7) (2012) 1144–1152.

[49] O. Shvydkiv, A. Yavorskyy, K. Nolan, A. Youssef, E. Riguet, N. Hoffmann, M. Oelgemöller, Photosensitized addition of isopropanol to furanones in a 365 nm UV-LED microchip, Photochem. Photobiol. Sci. 9 (2010) 1601–1603.

[50] A. Yavorskyy, O. Shvydkiv, N. Hoffmann, K. Nolan, M. Oelgemöller, Parallel microflow photochemistry: process optimization scale-up and library synthesis, Org. Lett. 14 (2012) 4342.

[51] O. Shvydkiv, C. Limburg, K. Nolan, M. Oelgemöller, Synthesis of juglone (5-hydroxy-1,4-naphthoquinone) in a falling film microreactor, J. Flow Chem. 2 (2012) 52–55.

[52] S.A.M.W. van den Broek, R. Becker, K. Koch, P.J. Nieuwland, Microreactor technology: real-time flow measurements in organic synthesis, Micromachines 3 (2012) 244–254.

[53] T. Aillet, K. Loubière, O. Dechy-Cabaret, L. Prat, Photochemical synthesis of a cage compound in a microreactor. rigorous comparison with a batch photoreactor, Chem. Eng. Process. Process Intensif. 64 (2013) 38–47.

[54] T. Aillet, K. Loubière, O. Dechy-Cabaret, L. Prat, Impact of the diffusion limitations in microphotoreactors, AIChE J. 61 (4) (2015) 1284–1299.

[55] T. Aillet, K. Loubière, O. Dechy-Cabaret, L. Prat, Measurement of the photonic flux received inside a microphotoreactor by actinometry, Int. J. Chem. React. Eng. 12 (1) (2014) 1–13.

[56] T. Aillet, K. Loubière, O. Dechy-Cabaret, L. Prat, Microreactors as a tool for acquiring kinetics data on photochemical reactions, Chem. Eng. Technol. 39 (1) (2016) 115–122.

[57] W.A. Fiveland, Discrete-ordinates solutions of the radiative transport equation for rectangular enclosures, J. Heat Transfer. 106 (1984) 699–706.

[58] A. Peraiah, An Introduction to Radiative Transfer: Methods and Applications in Astrophysics, Cambridge University Press, New York, 2001.

[59] A.E. Cassano, C.A. Martin, R.J. Brandi, O.M. Alfano, Photoreactor analysis and design: fundamentals and applications, Ind. Eng. Chem. Res. 34 (1995) 2155–2201.

[60] A. Brucato, A. Cassano, F. Grisafi, G. Montante, L. Rizzuti, G. Vella, Estimating radiant fields in flat heterogeneous photoreactors by the six-flux model, AIChE J. 52 (2006) 3882–3890.

[61] G. Li Puma, A. Brucato, Dimensionless analysis of slurry photocatalytic reactors using a two-flux and six-flux radiation absorption-scattering models, Catal. Today 122 (2007) 78–90.

[62] J.-F. Cornet, C.-G. Dussap, A simple and reliable formula for assessment of maximum volumetric productivities in photobioreactors, Biotechnol. Prog. 25 (2009) 424–435.

[63] P.J. Valades-Pelayo, J. Moreira, B. Serrano, H. de Lasa, Boundary conditions and phase functions in a Photo-CREC Water-II reactor radiation field, Chem. Eng. Sci. 107 (2014) 123–136.

[64] Y. Boyjoo, M. An, V. Pareek, CFD simulation of a pilot scale slurry photocatalytic reactor and design of multiple-lamp reactors, Chem. Eng. Sci. 111 (2014) 266–277.

[65] A.E. Cassano, P.L. Silveston, J.M. Smith, Photochemical reaction engineering, Ind. Eng. Chem. 59 (1) (1967) 18–38.

[66] J.C. Andre, M.L. Viriot, A. Saïd, Industrial photochemistry XI: comparison between different types of photoreactors and selective filtering for monomolecular photoreactions, J. Photochem. Photobiol. Chem. 42 (2–3) (1988) 383–396.

[67] A. Bouchy, J.C. Andre, E. George, M.L. Viriot, Industrial photochemistry XIII: determination of the most suitable irradiation conditions for molecular photoreactions, J. Photochem. Photobiol. Chem. 48 (2–3) (1989) 447–463.

[68] N. Midoux, C. Roizard, J.C. Andre, Industrial photochemistry XVII: macroscopic transport effects on the performance of photochemical reactors, J. Photochem. Photobiol. Chem. 58 (1) (1991) 71–97.

[69] M. Mohajerani, M. Mehrvar, F. Ein-Mozaffari, Photoreactor design and CFD modelling of a UV/H_2O_2 process for distillery wastewater treatment, Can. J. Chem. Eng. 90 (3) (2012) 719–729.

[70] M. Mohajerani, M. Mehrvar, F. Ein-Mozaffari, CFD Modeling of metronidazole degradation in water by the UV/H_2O_2 process in single and multilamp photoreactors, Ind. Eng. Chem. Res. 49 (11) (2010) 5367–5382.

[71] S. Elyasi, F. Taghipour, Performance evaluation of UV reactor using optical diagnostic techniques, AIChE J. 57 (1) (2011) 208–217.

[73] J.-F. Cornet, Calculation of optimal design and ideal productivities of volumetrically lightened photobioreactors using the constructal approach, Chem. Eng. Sci. 65 (2) (2010) 985–998.

[74] T. Aillet, K. Loubière, O. Dechy-Cabaret, L. Prat, Impact of photon and mass transfer on photochemical reaction output in small-scale flow systems, 13th International Conference on Microreaction Technology (IMRET13), Budapest, June 2014, 2014.